GSC Advanced Research and Reviews
eISSN: 2582-4597 CODEN (USA): GARRC2
Cross Ref DOI: 10.30574/gscarr
Journal homepage: https://gscarr.gsconlinepress.com/

(RESEARCH ARTICLE)

ANTIBACTERIAL ACTIVITY OF SILVER NANOPARTICLES AGAINST *KLEBSIELLA PNEUMONIA*E THAT ISOLATED FROM BURN PATIENTS

Tuqa. A. Al-Kateeb and Alaa K. hameed *

Department of biology, College of Science, Al-Qasim Green University, Babylon 51013, Iraq.
* Corresponding Author

ORCID Details
Alaa K. hameed: https://orcid.org/0000-0002-1379-4036

GSC Advanced Research and Reviews, 2026, 28(02), 074–082

Publication history: Received on 04 July 2026; revised on 12 August 2026; accepted on 14 August 2026

Article DOI: https://doi.org/10.30574/gscarr.2026.28.2.0190

ABSTRACT

Background: *Klebsiella pneumoniae* is an opportunistic pathogen notorious for causing life-threatening infections in immunocompromised patients, primarily due to its antiphagocytic polysaccharide capsule. Hypervirulent strains exhibiting a hypermucoviscous phenotype further complicate this scenario by triggering invasive infections even in healthy individuals. In burn-wound settings, this pathogen remains a leading cause of colonization and sepsis. Given the rising challenges of antimicrobial resistance, silver nanoparticles (AgNPs) have gained attention as alternative therapeutic agents with dual antibacterial and antibiofilm properties. However, data regarding the prevalence of hypervirulent *K. pneumoniae* in burn wounds and the efficacy of AgNPs against such clinical isolates remain limited.

Methods: A total of 100 clinical burn-wound samples were collected from November 2025 to February 2026. *K. pneumoniae* was isolated and identified using conventional culture, biochemical tests, and the VITEK 2 Compact system, while hypermucoviscous strains were screened via the string test. The synthesized AgNPs were characterized using UV-Vis spectroscopy, SEM, XRD, FT-IR, and AFM. Their antibacterial activity was evaluated at concentrations of 1, 0.5, 0.25, and 0.12 mg/mL, and their anti-biofilm activity was assessed using the microtiter-plate method.

Results: *K. pneumoniae* was recovered from 35 out of 100 burn-wound samples (35%), with 80% (28/35) of isolates testing positive for the hypermucoviscous phenotype via the string test. The synthesized AgNPs exhibited a surface plasmon resonance peak at 406 nm, spherical morphology with an average size of 35 nm, face-centered cubic crystalline reflections, and particle heights of 41.67–44.91 nm. Antibacterial activity was concentration-dependent, with mean inhibition zones of 30.3, 25.8, 20.7, and 16.0 mm at 1, 0.50, 0.25, and 0.12 mg/mL, respectively, while anti-biofilm activity was observed across all concentrations and was maximal at higher doses.

Conclusion: The present findings reveal a considerable frequency of the hypermucoviscous phenotype among *K. pneumoniae* clinical isolates derived from burn wounds. Concurrently, the synthesized AgNPs demonstrated notable antibacterial and antibiofilm potential in a concentration-dependent manner. Despite these promising in vitro outcomes, the therapeutic deployment of these nanoparticles requires comprehensive preclinical and clinical evaluation, with particular emphasis on safety profiling, mechanistic pathways, and in vivo efficacy.

Keywords: *Klebsiella Pneumoniae*; Burn-Wound Infection; Hypermucoviscous Phenotype; Silver Nanoparticles; Antibacterial Activity; Biofilm Inhibition

1 INTRODUCTION

As a prominent opportunistic Gram-negative pathogen, *Klebsiella pneumoniae* is implicated in a broad array of clinical infections, spanning both hospital-acquired and community-onset cases. The progressive proliferation of multidrug-resistant variants of this microorganism has risen to the forefront of international public health priorities. Both the World Health Organization and the Centers for Disease Control and Prevention have classified it as an urgent antimicrobial resistance threat, given its strong association with increased mortality, significant morbidity, and unfavorable clinical trajectories [1,2]. The pathogenic landscape of *K. pneumoniae* is shaped by a repertoire of virulence-associated factors, chiefly the lipopolysaccharide capsule, fimbrial structures, and siderophores, which synergistically enhance bacterial adherence, invasive potential, colonization efficiency, and resistance to phagocytosis [3]. In contrast to its classical counterparts, the hypervirulent lineage (hvKp) is defined by an accentuated virulence profile and a marked ability to provoke systemic invasive infections, including in otherwise healthy individuals [4,5].

Among the repertoire of virulence attributes characterizing hypervirulent *Klebsiella pneumoniae*, the capsular polysaccharide occupies a preeminent position, serving as the primary molecular determinant of its enhanced pathogenic phenotype[6]. This surface structure orchestrates a multifaceted immune evasion strategy, effectively subverting phagocytic clearance, abrogating complement-dependent opsonophagocytosis, and concurrently optimizing both local colonization and hematogenous spread to distant organs.

In the context of burn injuries, patients face an elevated infectious risk profile, stemming from compromised cutaneous defenses, protracted hospitalization periods, and the necessity for recurrent invasive procedures. The convergence of intrinsic antimicrobial resistance traits with hypervirulence-associated capsular features—particularly pronounced mucoviscosity—positions *K. pneumoniae* as a formidable adversary in burn units[7]. Accordingly, routine phenotypic screening for hypermucoviscous isolates may constitute a pragmatic approach to augmenting clinical decision-making and bolstering epidemiological monitoring initiatives.

The management of burn patients is inherently challenging, necessitating both specialized care and rigorous infection surveillance, driven by compromised skin integrity, prolonged hospitalization, and frequent invasive interventions. Within this vulnerable population, *K. pneumoniae* poses a significant threat, attributed to its multidrug resistance, capsular virulence factors, and robust biofilm formation. The escalating difficulty in managing refractory wound infections has accelerated the search for novel anti-infective agents. Silver nanoparticles (AgNPs) have attracted considerable interest due to their distinctive nanoscale properties and high surface reactivity, which are believed to induce membrane disruption, oxidative stress, and biofilm impairment. Nevertheless, AgNPs activity is critically influenced by particle size, aggregation, surface chemistry, concentration, and strain-dependent susceptibility. Accordingly, the present study was designed to integrate phenotypic profiling of K. pneumoniae from burn wounds with AgNPs characteriation and comprehensive evaluation of their antibacterial and antibiofilm potential[8].

2 MATERIAL AND METHODS

2.1 Study Design and Setting

A prospective cross-sectional investigation was executed within the Burn Unit of Hilla Teaching Hospital, located in Babil Governorate, Iraq, spanning the period from November 2025 to February 2026.

2.2 Specimen Collection

Individual wound swab samples were procured employing standardized aseptic techniques, wherein a sterile swab was systematically applied across the wound surface. Collected specimens were promptly conveyed to the microbiology facility for comprehensive bacteriological processing.

2.3 Inclusion and Exclusion Criteria

2.3.1 Inclusion criteria

The study population comprised all burn patients admitted to the burn unit throughout the study duration, encompassing both genders and all age categories, who exhibited clinical evidence of wound infection and underwent wound swabbing for diagnostic microbiological examination.

2.3.2 Exclusion criteria

Patient exclusion was applied under the following circumstances: refusal to participate, inability to obtain informed consent, specimens demonstrating no bacterial proliferation on culture, contaminated or otherwise inadequate samples, and duplicate specimens procured from a single patient—wherein solely the primary isolate was incorporated into the study analysis.

2.4 Laboratory Procedures

A total of 100 wound specimens were collected from burn patients and processed for bacterial isolation and identification. *K. pneumoniae* isolates were identified using a combination of biochemical tests (indole production, oxidase, catalase, urease activity, and Simmons citrate utilization), culture on selective and differential media, the string test, and the VITEK® 2 Compact system (bioMérieux, France).

2.5 Isolation and Identification of Isolates

Standard microbiological methods were employed for the isolation and identification of *K. pneumoniae* [9]. Wound swabs obtained from burn patients were inoculated into Brain Heart Infusion (BHI) broth and subsequently subcultured onto MacConkey agar, Blood agar, and Eosin Methylene Blue (EMB) agar [10]. All plates were incubated aerobically at 37°C for 24 hours.

Gram staining was performed to confirm the presence of Gram-negative bacilli. The hypermucoviscosity phenotype was assessed using the string test, in which a bacteriological loop is used to stretch a colony; a positive result is indicated by the formation of a viscous string measuring ≥5 mm in length. All presumptive isolates were further confirmed using the VITEK® 2 Compact system (bioMérieux, France) [11].

2.6 Silver Nanoparticle Characterization and Antimicrobial Assays

2.6.1 Characterization of Silver Nanoparticles

The synthesized silver nanoparticles (AgNPs) were characterized using a range of complementary analytical techniques, including ultraviolet-visible (UV-Vis) spectroscopy, scanning electron microscopy (SEM), X-ray diffraction (XRD), Fourier-transform infrared (FT-IR) spectroscopy, and atomic force microscopy (AFM). These methods were employed to evaluate the optical properties, surface morphology, crystalline structure, surface-associated functional chemical groups, and particle height of the AgNPs [12].

2.6.2 Antibacterial Activity Assay

The antibacterial efficacy of the AgNPs was evaluated against the recovered *K. pneumoniae* isolates at concentrations of 1, 0.5, 0.25, and 0.12 mg/mL. The resulting zones of inhibition were measured and compared with those produced by selected reference antibiotics, including imipenem, amikacin, gentamicin, and ceftriaxone[13].

2.6.3 Anti-biofilm Activity Assay

The anti-biofilm activity of the AgNPs was assessed using a microtiter plate-based method at concentrations of 1, 0.5, 0.25, and 0.125 mg/mL. Absorbance readings were recorded, and the percentage of biofilm inhibition was calculated for each of the tested isolates[14].

2.7 Statistical Analysis

Data were expressed as mean ± SD from triplicate experiments. One-way ANOVA followed by Tukey's post-hoc test compared AgNP concentrations. IC50 for biofilm inhibition was calculated by nonlinear regression. Susceptibility was defined per CLSI guidelines (inhibition zones ≥16 mm). Fisher's Exact Test compared susceptibility proportions, with OR and 95% CI calculated. $P < 0.05$ was significant.

3 RESULTS AND DISCUSSION

Klebsiella pneumoniae accounted for 35% (n=35) of the 100 clinical specimens collected as shown in Figure 1. The hypermucoviscous (HMV) phenotype, determined via the string test, was observed in 28 of these isolates (80%) as per Table 1, which produced a viscous filament exceeding 5 mm in length upon loop stretching, while the remaining 7 isolates (20%) did not exhibit this trait [15,16].

Figure 1: *Klebsiella pneumoniae* colonies on EMB agar, MacConkey agar, and blood

Table 1: Distribution of *K.pneumoniae* Isolates According to the String Test

String Test Result	String Test Characteristics	Number (N=35)	Percentage (%)
Hypermucoviscous (Positive)	>5 mm	28	80%
Non-Hypermucoviscous (Negative)	≤5 mm	7	20%
Total		35	100

The synthesized silver nanoparticles (AgNPs) were characterized using multiple analytical techniques. UV-Vis absorption spectroscopy revealed a Surface Plasmon Resonance (SPR) band at approximately 406 nm with an absorbance of 0.91, characteristic of spherical silver nanoparticles Figure 2. The broad nature of the absorption band indicated a polydisperse size distribution and partial aggregation within the colloidal suspension Figure 2 [17].

Scanning electron microscopy (SEM) analysis confirmed that the AgNPs were predominantly spherical with an average particle size of 35 nm (range 20–60 nm) and limited aggregation, consistent with previous reports Figure 2 [18] . X-ray diffraction (XRD) revealed four major peaks at 38.1°, 44.3°, 64.4°, and 77.4°, corresponding to the (111), (200), (220), and (311) planes of a face-centered cubic (FCC) crystalline structure (JCPDS 04-0783), with the highest intensity at the (111) plane confirming preferential crystal growth and high phase purity Figure 2. Fourier-transform infrared (FT-IR) spectroscopy showed bands at 3699.82, 3175.74, 1382.94, and 832.80 cm^{-1}, attributed to O–H stretching, residual nitrate vibrations, and Ag–O stretching, respectively, confirming successful AgNP synthesis with minimal organic residues Figure 2. Atomic force microscopy (AFM) revealed particle heights ranging from 41.67 to 44.91 nm over a 5×5 µm scan area, confirming nanoscale dimensions consistent with SEM observations Figure 2 [19].

The antibacterial activity of AgNPs against *K. pneumoniae* isolates was evaluated at concentrations of 1, 0.5, 0.25, and 0.12 mg/mL. At 1 mg/mL, all isolates showed complete growth inhibition, while at 0.5 mg/mL, significant inhibition was observed. At 0.25 and 0.12 mg/mL, weak to moderate inhibition was recorded with no significant differences, identifying 1 mg/mL as the most effective concentration [20]. The comparative activity of AgNPs against multi-drug resistant (MDR) *K. pneumoniae* isolates demonstrated a dose-dependent increase in antibacterial efficacy, with mean inhibition zones of 30.3 ± 5.8 mm (1 mg/mL), 25.8 ± 5.2 mm (0.5 mg/mL), 20.7 ± 4.3 mm (0.25 mg/mL), and 16.0 ± 4.1 mm (0.12 mg/mL) Table 2[21].

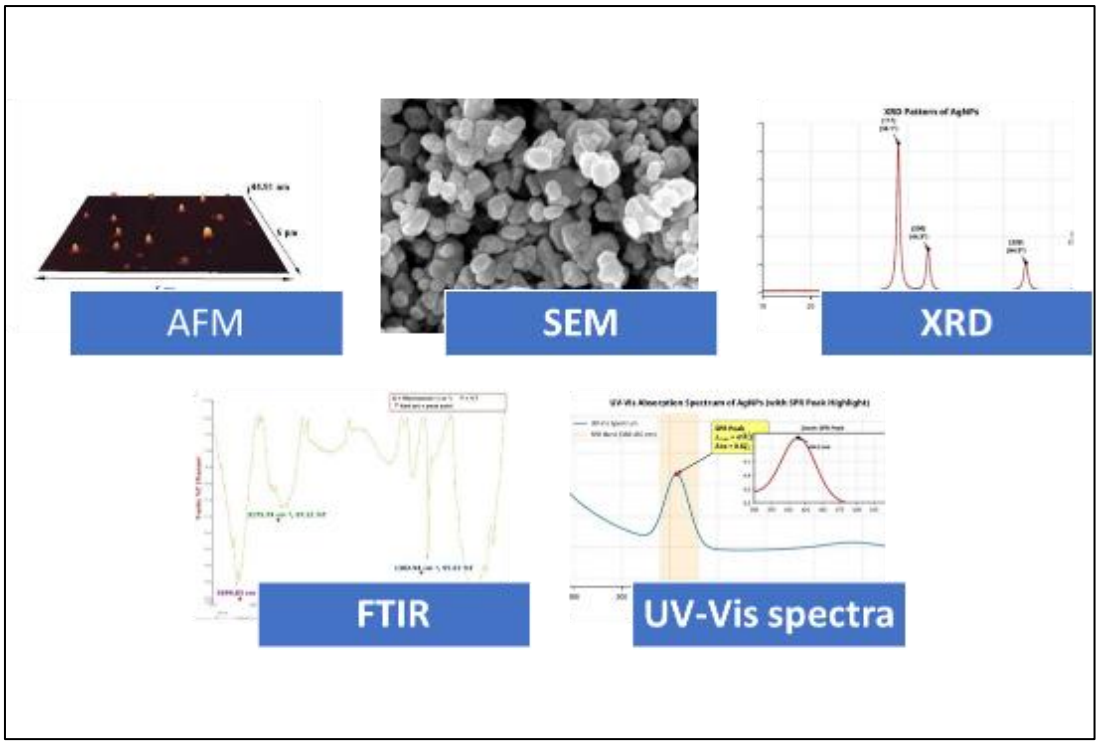

Figure 2: **Physicochemical characterization of AgNPs: (A) AFM, (B) SEM, (C) XRD pattern, (D) UV-Vis absorption spectrum showing surface plasmon resonance (SPR) peak at 411.2 nm, and (E) FTIR spectrum.**

Table 2: **Descriptive Statistics of Inhibition Zones (mm) Produced by AgNPs and Antibiotics Against MDR *K. pneumoniae* Isolates**

Parameter	AgNPs 1	AgNPs 0.5	AgNPs 0.25	AgNPs 0.12	IPM (10)	AK (30)	CN (30)	CTR (30)
Mean ± SD	30.3 ± 5.8	25.8 ± 5.2	20.7 ± 4.3	16.0 ± 4.1	20.7 ± 4.5	17.0 ± 3.9	14.3 ± 5.1	9.2 ± 7.4
Median	30	25	20	15	20	16	15	11
Mode	30	25	20	18	20	16	15	0
Range	17-35	16-34	15-26	22-Oct	15-30	25-Dec	0-25	0-22
CV (%)	19.1	20.2	20.8	25-Jan	21.7	22-Jan	35.7	80.4

*SD: Standard Deviation; CV: Coefficient of Variation.

Concentrations of 1, 0.5, and 0.25 mg/mL achieved 100% susceptibility among the tested isolates Table 3. Statistical analysis revealed that AgNPs at 1 mg/mL were significantly more effective than gentamicin (CN) (OR = 0.46; P < 0.001) and ceftriaxone (CTR) (OR = 0.23; P < 0.001), while AgNPs at 0.25 mg/mL showed comparable efficacy to imipenem (IPM) (P = 0.492) Table 4. These findings highlight the potential of AgNPs as promising alternatives against MDR isolates, including carbapenem-resistant strains [22,23].

Table 3: Association Between Treatments and Susceptibility Using Fisher's Exact Test and Odds Ratio (OR) with 95% Confidence Interval (CI).

Treatment	Susceptible n (%)	Resistant n (%)	Odds Ratio (OR)	95% CI	P-value (Fisher's Exact)
AgNPs 1	35 (100%)	0 (0.0%)		-	-
AgNPs 0.5	35 (100%)	0 (0.0%)	1	0.98 - 1.02	1
AgNPs 0.25	35 (100%)	0 (0.0%)	1	0.98 - 1.02	1
AgNPs 0.12	32 (91.4%)	3 (8.6%)	0.91	0.82 - 0.99	0.238
IPM (10)	33 (94.3%)	2 (5.7%)	0.94	0.86 - 1.02	0.492

AK (30)	30 (85.7%)	5 (14.3%)	0.86	0.74 - 0.98	0.049*
CN (30)	16 (45.7%)	19 (54.3%)	0.46	0.31 - 0.64	< 0.001*
CTR (30)	8 (22.9%)	27 (77.1%)	0.23	0.13 - 0.38	< 0.001*

*Susceptible defined as inhibition zone ≥ 16 mm; Resistant defined as inhibition zone < 16 mm according to CLSI guidelines (M100, 2023). OR calculated relative to AgNPs 1 as reference. Statistically significant (P < 0.05).

Table 4: Association Between AgNP Concentrations and Antibiotic Resistance Using Fisher's Exact Test

Comparison	Susceptible (AgNPs) n (%)	Resistant (AgNPs) n (%)	OR	95% CI	P-value
AgNPs 1 vs AgNPs 0.5	35 vs 35 (100%)	0 vs 0 (0%)	1	0.98 - 1.02	1
AgNPs 1 vs AgNPs 0.25	35 vs 35 (100%)	0 vs 0 (0%)	1	0.98 - 1.02	1
AgNPs 1 vs AgNPs 0.12	35 vs 32 (91.4%)	0 vs 3 (8.6%)	0.91	0.82 - 0.99	0.238
AgNPs 1 vs IPM	35 vs 33 (94.3%)	0 vs 2 (5.7%)	0.94	0.86 - 1.02	0.492
AgNPs 1 vs AK	35 vs 30 (85.7%)	0 vs 5 (14.3%)	0.86	0.74 - 0.98	0.049*
AgNPs 1 vs CN	35 vs 16 (45.7%)	0 vs 19 (54.3%)	0.46	0.31 - 0.64	< 0.001*
AgNPs 1 vs CTR	35 vs 8 (22.9%)	0 vs 27 (77.1%)	0.23	0.13 - 0.38	< 0.001*
AgNPs 0.5 vs IPM	35 vs 33 (94.3%)	0 vs 2 (5.7%)	0.94	0.86 - 1.02	0.492
AgNPs 0.5 vs AK	35 vs 30 (85.7%)	0 vs 5 (14.3%)	0.86	0.74 - 0.98	0.049*
AgNPs 0.5 vs CN	35 vs 16 (45.7%)	0 vs 19 (54.3%)	0.46	0.31 - 0.64	< 0.001*
AgNPs 0.5 vs CTR	35 vs 8 (22.9%)	0 vs 27 (77.1%)	0.23	0.13 - 0.38	< 0.001*
AgNPs 0.25 vs IPM	35 vs 33 (94.3%)	0 vs 2 (5.7%)	0.94	0.86 - 1.02	0.492
AgNPs 0.25 vs AK	35 vs 30 (85.7%)	0 vs 5 (14.3%)	0.86	0.74 - 0.98	0.049*
AgNPs 0.25 vs CN	35 vs 16 (45.7%)	0 vs 19 (54.3%)	0.46	0.31 - 0.64	< 0.001*
AgNPs 0.25 vs CTR	35 vs 8 (22.9%)	0 vs 27 (77.1%)	0.23	0.13 - 0.38	< 0.001*
IPM vs AK	33 (94.3%) vs 30 (85.7%)	2 (5.7%) vs 5 (14.3%)	0.91	0.82 - 1.01	0.427
IPM vs CN	33 (94.3%) vs 16 (45.7%)	2 (5.7%) vs 19 (54.3%)	0.48	0.33 - 0.67	< 0.001*
IPM vs CTR	33 (94.3%) vs 8 (22.9%)	2 (5.7%) vs 27 (77.1%)	0.24	0.14 - 0.39	< 0.001*
AK vs CN	30 (85.7%) vs 16 (45.7%)	5 (14.3%) vs 19 (54.3%)	0.53	0.38 - 0.72	< 0.001*
AK vs CTR	30 (85.7%) vs 8 (22.9%)	5 (14.3%) vs 27 (77.1%)	0.27	0.16 - 0.43	< 0.001*
CN vs CTR	16 (45.7%) vs 8 (22.9%)	19 (54.3%) vs 27 (77.1%)	0.5	0.34 - 0.72	0.052

The anti-biofilm activity of AgNPs was evaluated using the microtiter plate method. Biofilm inhibition was concentration-dependent, with mean inhibition percentages of 52.18 ± 6.12%, 48.95 ± 7.84%, 32.41 ± 14.23%, and 24.87 ± 15.96% at 1, 0.5, 0.25, and 0.125 mg/mL, respectively Table 4 [24]. The IC50 was calculated as 0.42 mg/mL, and overall inhibition rates were 91.4%, 85.7%, 71.4%, and 51.4% at the respective concentrations (P < 0.001 to <0.05) Table 5. These results are consistent with previous studies confirming the anti-biofilm potential of AgNPs against *K. pneumoniae* through multiple mechanisms, including oxidative stress induction and biofilm architecture disruption[25, 26].

Table 5: Anti-biofilm activity of silver nanoparticles against *K.pneumoniae* isolates

Concentration (mg/mL)	Total Isolates	Mean Inhibition (%) ± SD	Minimum Inhibition (%)	Maximum Inhibition (%)	Inhibition Isolates (%)	Non-inhibition Isolates (%)	P-value
1	35	52.18 ± 6.12	41.62	62.28	32 (91.4%)	3(8.6%)	< 0.001
0.5	35	48.95 ± 7.84	38.08	61.55	30(85.7%)	5(14.3%)	< 0.001
0.25	35	32.41 ± 14.23	11.77	51.05	25 (71.4%)	10(28.6%)	< 0.01
0.125	35	24.87 ± 15.96	1.73	45.77	18 (51.4%)	17 (48.6%)	< 0.05
IC50	%100	0.42 mg/mL	-	-	-		

*OR: Odds Ratio; CI: Confidence Interval. Susceptible defined as inhibition zone ≥ 16 mm; Resistant defined as inhibition zone < 16 mm. Statistically significant (P < 0.05).

4 CONCLUSION

Silver nanoparticles (AgNPs) (~35 nm) were successfully synthesized and demonstrated potent, dose-dependent antibacterial activity against *K. pneumoniae* isolates, with complete growth inhibition at 1 mg/mL. AgNPs outperformed gentamicin and ceftriaxone and matched imipenem at lower concentrations, positioning them as promising alternatives against MDR and carbapenem-resistant strains. They also exhibited significant anti-biofilm activity (up to 91.4% inhibition; IC50 = 0.42 mg/mL). In conclusion, AgNPs are dual-action anti-infective agents warranting further in vivo and clinical studies as potential adjuncts or alternatives to conventional antibiotics.

STATEMENTS ON COMPLIANCE WITH ETHICAL STANDARDS

Disclosure of conflict of interest

The authors report no conflicts of interest

Statement of ethical approval

This study was approved by the Research Ethics Committee of Al-Qasim Green University in coordination with the Training and Development Department of the Babil Health Directorate (Approval No. QGEC/59, dated 22 October 2025). The study was conducted in accordance with the ethical principles of the Declaration of Helsinki.

Statement of informed consent

Written informed consent was obtained from all participants or their legal guardians before sample collection.

REFERENCES

[1] Li Y, Kumar S, Zhang L, Wu H, Wu H. Characteristics of antibiotic resistance mechanisms and genes of Klebsiella pneumoniae. Open Med (Wars). 2023;18(1):20230707. https://doi.org/10.1515/med-2023-0707

[2] Riwu KHP, Effendi MH, Rantam FA, Khairullah AR, Widodo A. A review: Virulence factors of Klebsiella pneumoniae as emerging infection on the food chain. Vet World. 2022;15(9):2172-2179 https://doi.org/10.14202/vetworld.2022.2172-2179

[3] Wang Q, Yu H, Pan X, et al. Exploring current hypervirulent Klebsiella pneumoniae infections: insights into pathogenesis, drug resistance, and vaccine prospects. Front Microbiol. 2025;16:1604763. https://doi:10.3389/fmicb.2025.1604763

[4] Guo Y, Wang S, Zhan L, et al. Microbiological and clinical characteristics of hypermucoviscous Klebsiella pneumoniae isolates associated with invasive infections in China. Front Cell Infect Microbiol. 2017;7:24. https://doi.org/10.3389/fcimb.2017.00024

[5] 5-Zhu J, Wang T, Chen L, Du H. Virulence factors in hypervirulent Klebsiella pneumoniae. Front Microbiol. 2021;12:642484. https://doi.org/10.3389/fmicb.2021.642484.

[6] Tiria, F., Odoyo, E., Georges, M., Nyerere, A., & Musila, L. (2023). Molecular detection of key virulence-associated genes and phenotypic analysis of virulence traits of Klebsiella pneumoniae clinical isolates from Kenya. Journal of Pure and Applied Microbiology, *17*(4), 2194–2204. https://doi.org/10.22207/JPAM.17.4.16

[7] Rajabloo, Z., Mobarak Qamsari, E., & Kasra Kermanshahi, R. (2025). Identification and determining the pattern of antibiotic resistance and biofilm formation capacity in bacterial strains isolated from patients with burn wound infection. aumj, 14(2), 140–153. http://aums.abzums.ac.ir/article-1-1857-en.html

[8] Alhadrami, Hani A., Elswifi, Gamal H., Rateb, Mostafa E., Hamd, Ahmed, Insights on Silver Nanoparticles as Potential Antibacterial, Antibiofilm, and Photocatalytic Candidate: Experimental and Computational Approaches, Journal of Chemistry, 2025, 5511078, 15 pages, 2025. https://doi.org/10.1155/joch/5511078

[9] Bahy R, Fatyan E, Saafan AE, El-Gebaly EAE. Preparation and evaluation of a new combined conjugated vaccine against Klebsiella pneumoniae and Pseudomonas aeruginosa. J Appl Microbiol. 2022;133(3):1543-1554. https://doi.org/10.1111/jam.15673

[10] Rawy DK, El-Mokhtar MA, Hemida SK, Askora A, Yousef N. Isolation, characterization and identification of Klebsiella pneumoniae from Assiut University Hospital and sewage water in Assiut Governorate, Egypt. Assiut Univ J Bot Microbiol. 2020;49(2):60-76.

[11] Kumabe A, Kenzaka T. String test of hypervirulent Klebsiella pneumoniae. QJM. 2014;107(12):1053. https://doi.org/10.1093/qjmed/hcu124

[12] Li, H., Yang, Z., Khan, S. A., Walsh, L. J., Seneviratne, C. J., & Ziora, Z. M. (2024). Characteristics of metallic nanoparticles (especially silver nanoparticles) as anti-biofilm agents. Antibiotics, *13*(9), 819. https://doi.org/10.3390/antibiotics13090819

[13] Fontoura, I., & Castilho, M. L. (2026). Electrokinetic and Antibiofilm Effects of Silver Nanoparticles Combined with Imipenem Against multidrug-resistant of Klebsiella pneumoniae. IEEE transactions on nanobioscience, PP, 10.1109/TNB.2026.3699974. Advance online publication. https://doi.org/10.1109/TNB.2026.3699974

[14] El-Telbany, M., & El-Sharaki, A. (2022). Antibacterial and anti-biofilm activity of silver nanoparticles on multi-drug resistance pseudomonas aeruginosa isolated from dental-implant. Journal of oral biology and craniofacial research, 12(1), 199–203. https://doi.org/10.1016/j.jobcr.2021.12.002

[15] Thapa, T. B., Maharjan, S., Giri, N., Sapkota, M., Shrestha, O., Khanal, P. R., & Joshi, G. (2025). Incidence of hypermucoviscous Klebsiella pneumoniae and phenotypic detection of their virulence factors along with classical strains among patients visiting tertiary care hospital. Journal of infection in developing countries, 19(2), 258–266. https://doi.org/10.3855/jidc.19456

[16] Khairuddin, A., Nik Zuraina, N. M. N., Mohamad Nasir, N. S., Chua, W. C., Abdul Halim, H. S., Yusof, W., Hussin, A., Yean Yean, C., & Hassan, S. A. (2025). Microbiological and clinical characteristics of hypervirulent Klebsiella pneumoniae isolated from patients in tertiary centers: A retrospective study. PeerJ, 13, e20198. https://doi.org/10.7717/peerj.20198

[17] Chirumamilla, P., Dharavath, S. B., & Taduri, S. (2023). Eco-friendly green synthesis of silver nanoparticles from leaf extract of Solanum khasianum: Optical properties and biological applications. Applied Biochemistry and Biotechnology, *195*(1), 353–368. https://doi.org/10.1007/s12010-022-04156-4

[18] Khatoon, U. T., Rao, K. V., Rao, J. V. R., & Aparna, Y. (2011). Synthesis and characterization of silver nanoparticles by chemical reduction method. In 2011 International Conference on Nanoscience, Engineering and Technology (ICONSET 2011) (pp. 1-5). IEEE. https://doi.org/10.1109/iconset.2011.6167920

[19] Narayanan, K. B., & Park, H. H. (2014). Unnatural amino acid-mediated synthesis of silver nanoparticles and their antifungal activity against Candida species. Journal of Nanoparticle Research, *16*(8), Article 2523. https://doi.org/10.1007/s11051-014-2523-y

[20] Jiangyan Li, Lian Yu, Ruirui Wang, Jiaqi Lan, Ming Li, Yan Qiao, Zhaoyu Tao, Hezuo Lü, Fengchao Wang, Qiang Fang, Pu Guo, The role of silver nanoparticles alone and combined with imipenem on carbapenem-resistant Klebsiella pneumoniae, Journal of Applied Microbiology, Volume 135, Issue 5, May 2024, lxae077, https://doi.org/10.1093/jambio/lxae077

[21] Holubnycha, V. M., Korniienko, V. V., Husak, Y. V., Fedorenko, V. O., Tverezovska, O. I., Ivakhniuk, T. V., & Varava, Y. V. (2021). Antibacterial influence of silver nanoparticles on multi-resistant strains of K. pneumoniae isolated at hospitals. Eastern Ukrainian Medical Journal, *9*(4), 332–341. https://doi.org/10.21272/eumj.2021;9(4):332-341

[22] Naqvi, S. Z. H., Kiran, U., Ali, M. I., Jamal, A., Hameed, A., Ahmed, S., & Ali, N. (2013). Combined efficacy of biologically synthesized silver nanoparticles and different antibiotics against multidrug-resistant bacteria. International Journal of Nanomedicine, *8*, 3187–3195. https://doi.org/10.2147/IJN.S49284

[23] Mahfouz, A. M., Eraqi, W. A., El Hifnawi, H. N. E. D., Samir, R., & Ramadan, M. A. (2025). Genetic determinants of silver nanoparticle resistance and the impact of gamma irradiation on nanoparticle stability. BMC Microbiology, *25*(1), Article 18. https://doi.org/10.1186/s12866-024-03682-x

[24] Elashkar, E., Alfaraj, R., El-Borady, O. M., Amer, M. M., Algammal, A. M., & El-Demerdash, A. S. (2025). Novel silver nanoparticle-based biomaterials for combating Klebsiella pneumoniae biofilms. Frontiers in microbiology, 15, 1507274. https://doi.org/10.3389/fmicb.2024.1507274

[25] Fontoura, I., Veriato, T. S., Raniero, L. J., & Castilho, M. L. (2023). Analysis of capped silver nanoparticles combined with imipenem against different susceptibility profiles of Klebsiella pneumoniae. Antibiotics, *12*(3), 535. https://doi.org/10.3390/antibiotics12030535

[26] Mhavarkar, S. R., & Jadhav, S. B. (2025). Antibiofilm potential of silver nanoparticles from Mussaenda philippica mediated via reduction in AHLs activity against uropathogenic Klebsiella pneumoniae. South African Journal of Botany, *181*, 537–548. https://doi.org/10.1016/j.sajb.2025.04.040